DOI:10.1190/segam2020-3419338.1

Optimizing Distributed Acoustic Sensing (DAS) Acquisition: Test Well Design and Automated Data Analysis

Harold Merry[1], Weichang Li[1], Max Deffenbaugh[1], Andrey Bakulin[2]*
[1]Aramco Services Company, Aramco Research Center—Houston, 17155 Park Row, Houston, TX 77084
[2]EXPEC Advanced Research Center, Saudi Aramco. Dhahran, Saudi Arabia

Summary

As the benefit of distributed acoustic sensing (DAS) is proven in new applications from seismic data acquisition, reservoir and frac monitoring, and flow characterization, there is a need to optimize DAS survey design and acquisition parameters for each application. A fiber-optic test well was drilled to facilitate precision studies of the impact of acquisition choices on data quality. The effect of fiber type, packaging, and length, as well as the impact of acquisition parameters on data quality, has been investigated. To date, these experiments have produced nearly one thousand vertical seismic profile datasets with precision timing from common energy sources. An algorithm for automatic extraction of signal and noise spectra from these data has been developed to quantitatively characterize the effect of gauge length and leading cable length on the signal-to-noise ratio (SNR).

Introduction

Distributed acoustic sensing (DAS) using fiber optics has found its promising usage in an increasing number of applications, including seismic data acquisition (Daley et al 2013, Mateeva et al 2013, Daley et al 2016, Jousset et al 2018), reservoir monitoring (Mateeva et al 2013 and Mateeva et al 2014), and unconventional fracture characterization and monitoring (Jin and Roy 2017, Molenaar and Cox 2013). While, in theory, DAS provides several sensing advantages over traditional measurements in these applications, such as potentially extended coverage and high spatial resolution at a reasonable cost, there are numerous variables that impact the quality of DAS data. These begin with the signal bandwidth and amplitude, placement of fiber in the well and coupling, the range of the seismic sources, the geology around the well, the completion of the well, and DAS interrogator technology, DAS acquisition settings such as gauge length, pulse repetition rate, laser intensity, fiber characteristics including single or multi-mode fiber, reflectance of fiber, dielectric profile of fiber, the length of fiber and packaging of fiber within the conveyance cable/tube. In order to assess and obtain meaningful DAS solutions in these applications, a good understanding of the effect of these factors can be crucially important. While many of these effects have been heuristically known to the practitioners in each type of application, previously reported work on this topic has been few and of qualitative nature (Dean, Cuny and Hartog 2017, Pevzner et al 2018, Correa et al 2017). Here we describe fiber-optic testing well, instrumented with various types of DAS and geophones. We have completed an extensive set of tests at the well with various controlled configurations of acquisition parameters, which produced nearly one thousand vertical seismic profiles of identical timing. An automated analysis algorithm has been developed to efficiently process all these data, extracting signal and noise spectra from each gather, and quantitatively characterize the effect of gauge length and leading cable length on signal-to-noise ratio (SNR).

Well Design and DAS Installation

A fiber-optic instrumented test well was drilled to study how the quality of DAS data is influenced by these acquisition variables. The well is 1,500 ft deep and penetrates a sequence of sands and shales which provide measurable seismic reflections. Completed with a combination of steel and fiberglass, the well provides environments for conducting both cased-hole and open-hole measurements.

For validation, evaluation, and advanced research of fiber optic sensing, thirty-two (32) optical fibers of various types and packaging were cemented behind casing, as shown in Figure 1.

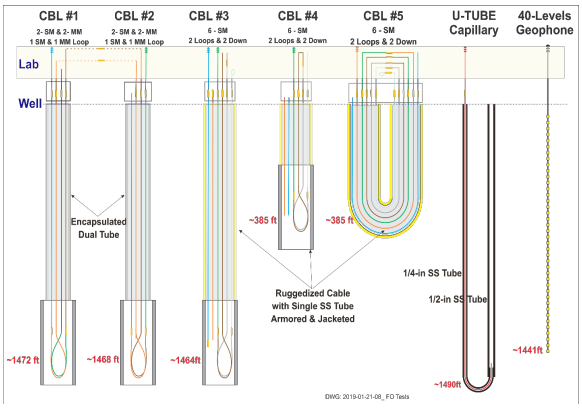

Figure 1. Sensing elements cemented behind casing in the fiber optic test well.

From Figure 1, cables #1 and #2 each contains two single-mode and two multi-mode CMTDA fibers within a traditional encapsulated dual tube. Both cables are terminated and looped at TD. Cables #3, #4 and #5 each contain six single-mode fibers within an inner tube, which is armored and jacketed for conveyance in the rugged

DOI:10.1190/segam2020-3419338.1

downhole environment. Cable #3 is terminated and looped at TD. Cable #4 is terminated and looped at 385 ft. Cable #5 is a dual looped cable at 385 ft.
For comparing and validating new types of engineered fibers, a capillary "U-tube" is cemented behind the casing where fibers can be easily pumped down, evaluated, and retrieved. For normalization of different sizes and strengths of seismic energy source and changing ground/geologic conditions utilized for various experimental programs, an array of 40 geophones is cemented behind casing from the surface to TD.

Acquisition Tests and Configuration

An extensive sequence of tests has been conducted at the fiber optic test well over the course of one year. One of the goals is to obtain a good understanding of the effects of various acquisition variables, and therefore to establish guidelines of good practice for effective field deployment. Here we present a subset of the tests which focus on the effects of varying DAS gauge length and length of the sensing fiber. The acquisition configuration for the example subset of the tests utilized in this paper is summarized in Table 1.

Utilizing two fiber loops from the same cable (CBL#3) behind the casing, we tested various configurations of two controlled acquisition variables, namely the gauge length and the length of the sensing cables.

Table 1. Summary of the focused subset of the DAS tests

The set of gauge length values vary from 16 m, 8 m, 4 m to 2 m. In addition, five lengths of lead-in cable length were tested, including 0', 5730', 11,450', 17,185' to 22,900', as illustrated in Figure 2.

Recording 2 fiber loops for each fiber length yielded two down-going legs and two up-going legs or 4 VSP datasets. Recording four different gauge lengths at each fiber length referred to as a "Set", yielded 16 VSP datasets. A total of 5x16=80 VSP datasets were acquired from five different fiber lengths and four different gauge length settings. For each VSP dataset, eight shots were acquired, producing a total of 80 x 8 = 640 shot records or samples for analysis.

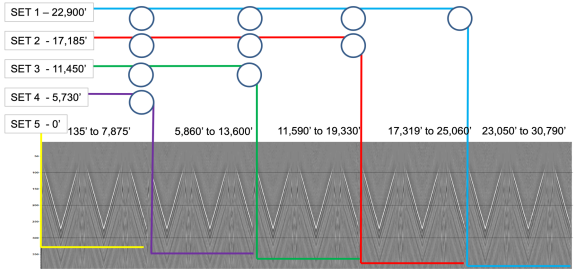

Figure 2. Five test groups of varying fiber lead-in lengths.

DOI:10.1190/segam2020-3419338.1

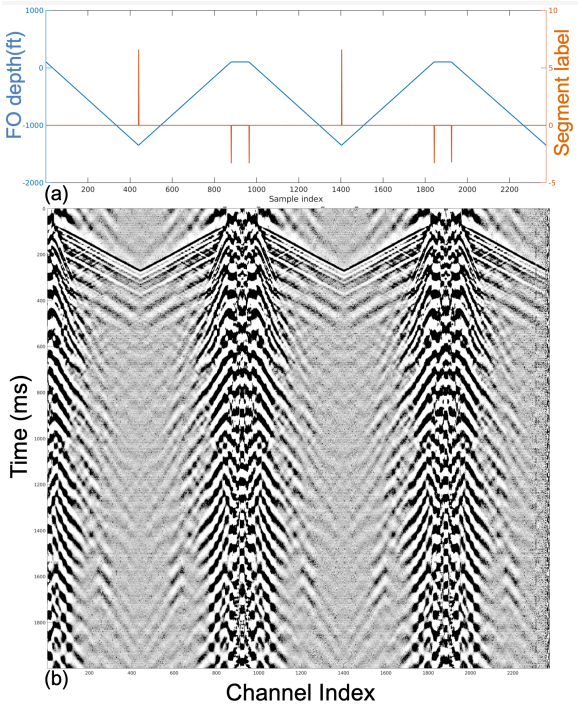

Figure 3. (a) Registered receiver depth and the extracted fold segment boundaries, and (b) the associated VSP shot with four up and down VSP datasets.

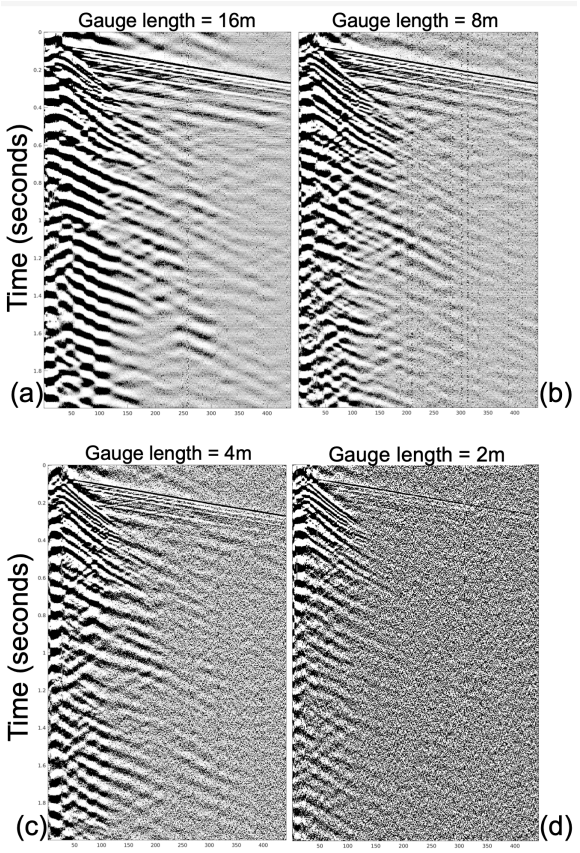

Figure 4. Comparison of individual VSP shot records with varying gauge length (a) 16 m, (b) 8 m, (c) 4 m, and (d) 2 m, at fixed fiber lead-in length of 23048.5'.

Data Analysis Method

With the vast amount of data collected from these tests, our objective is to quantitatively assess the effect of the acquisition variables. Specifically, we consider here the effect of the gauge length and the lead-in fiber length on DAS data quality as evaluated by the signal versus noise ratio over the signal bandwidth. The analysis consists of the following steps:

- Partition each shot record into individual VSP datasets;
- Pick first arrival for each VSP dataset;
- Extracting signal from flattened picked data;
- Extracting ambient noise prior to the picked arrival;
- Computing signal and noise spectra;
- Calculating SNR from the spectra by integrating over the signal bandwidth;
- Repeating computation over all the VSP datasets.

The raw VSP shots may have signals starting from different channel index due to varying lead-in cable lengths. We first align and then partition these VSP shots each corresponding to a dataset by a single up or down cable leg. This is achieved by using the receiver channel depth recorded during the tests.

Figure 3 illustrates the channel depth and the aligned and truncated VSP shot record as an example. The channel depth profile is twice differentiated to obtain the VSP dataset segment boundaries, which will be invariant to the fiber lead-in length. Each aligned VSP shot is then partitioned into five datasets along the segment boundaries. Records from the last up cable leg are significantly noisier due to cable end reflection and, therefore not used in the evaluation. Picking the arrival on the resulting VSP dataset is significantly easier than on the raw VSP shot. Figure 4 also shows the resulting VSP datasets obtained with four different gauge lengths while their lead-in cable lengths are the same. As shown, when the gauge length decreases from 16m, 8m, 4m to 2m, the signal strength degrades while the noise level increases significantly.

DOI:10.1190/segam2020-3419338.1

The rest of the steps are illustrated in Figure 5. For each VSP dataset, we pick the first arrival, as shown in Figure 5a, flatten the data following the picked arrival, and truncate it within a 168 ms x 364 channel window, and extract it as the signal component, shown in Figure 5c; then extract as the noise estimate from the record prior to the picked arrival (Figure 5b). The spectral amplitudes for the resulting signal and noise are plotted in Figure 5d, respectively. We then take squares of and integrate both spectra over the signal bandwidth [8 120] Hz to obtain the SNR ratio for the VSP dataset.

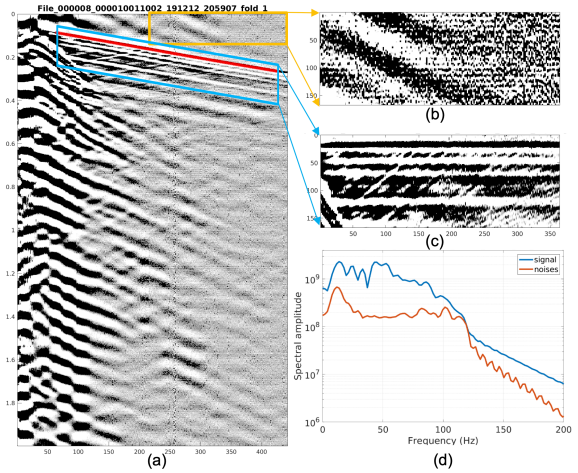

Figure 5. Single VSP processing: (a) pick first arrival (red line); capture part of the record prior to the picked arrival (yellow box) as ambient noise (b); and the flattened record following the picked arrival as the signal (c); the signal and noise spectra (d).

The same analysis is automated and then repeated over all the raw VSP shots, producing 640 SNR samples with different gauge length and fiber lead-in length configurations. Figure 6 shows the 3D scatter plot of all 640 samples. As shown, extending gauge length can increase the SNR level significantly, by 8 dB from 2 m to 4 m, 5 dB from 4 m to 8 m, and 2 dB from 8 m to 16 m, respectively, averaged over all the different lead-in length cases.

The effect of elongated fiber length can introduce degradation to the DAS signal and increase the noise level. As shown in Figure 6, reducing the lead-in fiber length from 30,000 feet to 0 can effectively increase SNR by as much as 12.5 dB in all cases with 2 m or 4 m gauge length. In the cases of 8 m and 16 m gauge length, the SNR gain from the same lead-in fiber length reduction is approximately 5 dB, indicating the averaging effect from long gauge length can potentially suppress the noise effect but not the signal degradation.

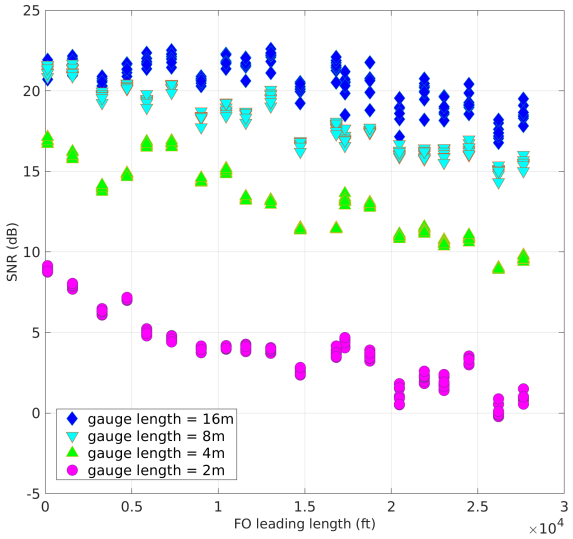

Figure 6. Signal-to-noise (SNR) as a function of the gauge length and lead-in cable length, integrated over [8, 120] Hz.

Conclusions

In this paper, we have presented a fiber-optic test well drilled to facilitate precision studies of the impact of acquisition choices on data quality. An extensive sequence of tests under controlled condition have been conducted at the well to investigate the effects of various acquisition variables. An automated analysis algorithm has been developed to process the large volume of DAS test data. The results have shown significant SNR variations over a range of gauge length from 2 to 16 meters and across lead-in cable length range from 30 thousand feet to hundred feet.

10.1190/segam2020-3419338.1

REFERENCES

Daley, T. M., B. M. Freifeld, J. Ajo-Franklin, S. Dou, R. Pevzner, V. Shulakova, S. Kashikar, D. E. Miller, J. Goetz, J. Henninges, and S. Lueth, 2013, Field testing of fiber-optic distributed acoustic sensing (DAS) for subsurface seismic monitoring: The Leading Edge, **32**: 699–706, doi: https://doi.org/10.1190/tle32060699.1.

Daley, T. M., D. E. Miller, K. Dodds, P. Cook, and B. M. Freifeld, 2016, Field testing of modular borehole monitoring with simultaneous distributed acoustic sensing and geophone vertical seismic profiles at Citronelle, Alabama: Field testing of MBM: Geophysical Prospecting, **64**, 1318–1334, doi: https://doi.org/10.1111/1365-2478.12324.

Mateeva, A., J. Mestayer, Z. Yang, J. Lopez, P. Wills, J. Roy, and T. Bown, 2013, Dual-well 3D VSP in deepwater made possible by DAS: 83rd Annual International Meeting, SEG, Expanded Abstracts, 5062–5066, doi: https://doi.org/10.1190/segam2013-0667.1.

Mateeva, A., J. Lopez, J. Mestayer, P. Wills, B. Cox, D. Kiyashchenko, Z. Yang, W. Berlang, R. Detomo, and S. Grandi, 2013. Distributed acoustic sensing for reservoir monitoring with VSP: The Leading Edge, **32**, 1278–1283, doi: https://doi.org/10.1190/tle32101278.1.

Mateeva, A., J. Lopez, H. Potters, J. Mestayer, B. Cox, D. Kiyashchenko, P. Wills, Z. Yang, W. Berlang, R. Detomo, and S. Grandi, 2014, Distributed acoustic sensing for reservoir monitoring with vertical seismic profiling: Distributed acoustic sensing (DAS) for reservoir monitoring with VSP: Geophysical Prospecting, **62**, 679–692, doi: https://doi.org/10.1111/1365-2478.12116.

Jin, G., and B. Roy, 2017, Hydraulic-fracture geometry characterization using low-frequency DAS signal: The Leading Edge, **36**, 975–980, doi: https://doi.org/10.1190/tle36120975.1.

Molenaar, M. M., and B. E. Cox, 2013, Field cases of hydraulic fracture stimulation diagnostics using fiber optic distributed acoustic sensing (DAS) measurements and analyses: SPE.

Jousset, P., T. Reinsch, T. Ryberg, H. Blanck, A. Clarke, R. Aghayev, G. P. Hersir, J. Henninges, M. Weber, and C. M. Krawczyk, 2018, Dynamic strain determination using fibre-optic cables allows imaging of seismological and structural features: Nature Communications, **9**, 1–11, doi: https://doi.org/10.1038/s41467-018-04860-y.

Aldawood, A., E. Alfataierge, and A. Bakulin, 2020, Introducing a new DAS test facility for evaluating emerging DAS technologies: EAGE, 1–5.

Bakulin, A., I. Silvestrov, and R. Pevzner, 2018, Surface seismic with DAS: Looking deep and shallow at the same time: 88th Annual International Meeting, SEG, Expanded Abstracts, 16–20, doi: https://doi.org/10.1190/segam2018-2995870.1.

Dean, T., T. Cuny, and A. H. Hartog, 2017, The effect of gauge length on axially incident P-waves measured using fibre optic distributed vibration sensing. Geophysical Prospecting, **65**, 184–193, doi: https://doi.org/10.1111/1365-2478.12419.

Pevzner, R., A. Bona, J. Correa, K. Tertyshnikov, G. Palmer, and O. Valishin, 2018, Optimising DAS VSP data acquisition parameters: Theory and experiments at curtin training well facility: EAGE.

Correa, J., A. Egorov, K. Tertyshnikov, A. Bona, R. Pevzner, T. Dean, B. Freifeld, and S. Marshall, 2017, Analysis of signal to noise and directivity characteristics of DAS VSP at near and far offsets — A CO2CRC Otway Project Data Example: The Leading Edge, **36**, 994a1–994a7, doi: https://doi.org/10.1190/tle36120994a1.1.

Ellmauthaler, A., M. Willis, D. Barfoot, X. Wu, C. Erdemir, O. Barrios-Lopez, D. Quinn, and S. Shaw, 2016, Depth calibration for DAS VSP: Lessons learned from two field trials: 86th Annual International Meeting, SEG, Expanded Abstracts, 632–636, doi: https://doi.org/10.1190/segam2016-13951487.1.

Spikes, K. T., N. Tisato, T. E. Hess, and J. W. Holt, 2019, Comparison of geophone and surface-deployed distributed acoustic sensing seismic data, geophone and surface DAS data: Geophysics, **84**, no. 2, A25–A29, doi: https://doi.org/10.1190/geo2018-0528.1.

Willis, M. E., C. Erdemir, A. Ellmauthaler, O. Barrios, and D. Barfoot, 2016, Comparing DAS and geophone zero-offset VSP data sets side-by-side: CSEG Recorder, **41**.